Journal of Fluorescence
https://doi.org/10.1007/s10895-020-02544-9

ORIGINAL ARTICLE

A Highly Efficient BODIPY Based Turn-off Fluorescent Probe for Detecting Cu^{2+}

Ruopei Sun[1] · Lusheng Wang[1] · Chao Jiang[1] · Ziyao Du[1] · Suwen Chen[1] · Wangsuo Wu[1]

Received: 27 February 2020 / Accepted: 23 April 2020

Abstract

Based on boron-dipyrromethene (BODIPY), taking 2-hydroxy-N-(2-hydroxyphenyl)benzamide as recognition site, a new fluorescent probe HHPBA-BODIPY aimed at sensitively detecting Cu ions was designed, synthesized and characterized.The emission spectra of HHPBA-BODIPY exhibited an intensive green fluorescence around 510 nm, with a maximum absorption near 500 nm. When Cu^{2+} ions are present, the fluorescence at 510 nm can be quenched with a good linearity between the copper ion concentrationand the fluorescence intensity and the detection limit is 0.35 μM. HHPBA-BODIPY is also selective toward Cu^{2+}, while other metal ions show no interfere except Fe^{3+} and Cr^{3+} ions. In addition, HHPBA-BODIPY also proved efficient to detect Cu^{2+} in water samples which offers the possibility to detect trace amount of Cu^{2+} for environmental monitoring. Copper ions; BODIPY; fluorescent probe.

Keywords BODIPY · Fluorescent probe · Copper ion detection · Cu^{2+}

Introduction

Cu^{2+} is an significant trace element and it acts as catalyst and structural cofactor for enzyme in a series of biochemical reactions and metabolic processes [1–4]. However, current evidences have pointed out that excessive intake of Cu^{2+} will increase the risk of neurological diseases including Parkinson's disease and Alzheimer disease [5–7]. In addition, Cu^{2+} is also a common pollutant for the fishery industry, and its toxicity will threaten the survival of many aquatic organisms [8–10]. Therefore, the rapid and simple analysis of trace Cu^{2+} is of great significance in environmental monitoring.

Comparing to traditional methods, fluorescence analysis has aroused extensive interests in various fields including biochemistry [11–13], analytical chemistry [14–16], diagnostics [17–19] and molecular biology [20–22] for its high selectivity, well sensitivity, simple analysis procedure and fast response. Up to now, a series of fluorescent probes based on coordination with Cu^{2+} have been designed and developed. Various chemical scaffolds such as rhodamine [23–27], naphthalimide [28, 29], dansyl derivatives [30, 31] were applied to design coordinative fluorescent probes and they exhibited excellent properties. Among these scaffolds, 4,4-difluoro-4-bora-3a,4a-diaza-s-indacence(BODIPY) perhaps is the highest potential candidate for its relative high molar absorption coefficients, high fluorescence quantum yields, resistance towards self-aggregation and high intensity emission peaks with narrow bandwidth. Furthermore, the spectroscopic properties of BODIPY can be controllably adjusted through various methods at appropriate positions [32–35]. Therefore, A fluorescent probe molecule HHPBA-BODIPY was synthesized by introducing amide receptors into the BODIPY framework, and phenolic hydroxyl and carbonyl groups were attached to the skeleton as donors, the coordination between Cu^{2+} and HHPBA-BODIPY resulted in changes of fluorescence absorption and emission spectra, which indicates the copper content in certain solutions. The fluorescence properties and the detective ability of HHPBA-BODIPY towards Cu^{2+} was investigated and evaluated in this work.

Experimental

Reagents

In this work all the reagents are of analytical level and used without any further purification. Cation solutions were

Electronic supplementary material The online version of this article (https://doi.org/10.1007/s10895-020-02544-9) contains supplementary material, which is available to authorized users.

✉ Suwen Chen
chensuwen@lzu.edu.cn

[1] School of Nuclear Science and Technology, Lanzhou University, 222 Tianshui South Rd, Chengguan District, Lanzhou, Gansu, China

prepared from $NaNO_3$, KNO_3, $Ca(NO_3)_2{\cdot}4H_2O$, $Mg(NO_3)_2{\cdot}6H_2O$, $Fe(NO_3)_3{\cdot}9H_2O$, $Cd(NO_3)_2{\cdot}4H_2O$, $Cr(NO_3)_3{\cdot}9H_2O$, $Zn(NO_3)_2{\cdot}6H_2O$, $Ni(NO_3)_2{\cdot}6H_2O$, $Co(NO_3)_2{\cdot}6H_2O$, $Ba(NO_3)_2$, $Pb(NO_3)_2$, $Al(NO_3)_3{\cdot}9H_2O$, $HgCl_2$. Deionized water was purified using distillation equipment. HEPES solution was prepared through solving calculated amount of solids in deionized water. Tap water and the Yellow River water were used as water samples. Yellow River water samples were used after being filtered with a 2.5 μm filter membrane, while tap water samples were used directly without any treatment. Column chromatography experiments were conducted over silica gel (200–300 mesh).

Apparatus

^1H NMR and ^{13}C NMR spectra were measured on Varian INOVA 600 MHz NMR spectrometer with TMS as internal standard. Ultraviolet-visible absorption spectra were measured by Perkin Elmer Lambda 35 spectrometer. High resolution mass spectra (HRMS) were obtained on a LTQ-Obitrap-ETD (Thermo Scientific) spectrometer, ESI-MS tests were conducted with a Bruker micrOTOF II spectrograph and fluorescence spectra were recorded by an Edingburgh Instruments FLS920 luminescence spectrometer. Absorption and emission spectra were measured in quartz cuvettes with 1 cm path length. The pH data of solutions were determined by a Sartorius pH meter.

Synthetic Procedures

Synthesis of T2 Compound T2 was prepared according to the reported procedure [36]. 836.3 mg 3-nitro-4-hydroxybenzaldehyde and 1 mL 2,4-dimethyl pyrrole were added into a 500 mL round-bottomed flask, 350 mL CH_2Cl_2 were introduced to the solution then. At room temperature this solution was stirred for 6-7 h in nitrogen atmosphere, then dichloromethane solution containing 1.2323 g tetrachlorobenzoquinone was introduced to the solution and then mixed for 30 min. Finally, a mixed solution of 6.6 mL diisopropylethylamine and 7.5 mL boron trifluoride ethyl ether was added to the solution slowly by using drop funnel, then further stir the mixture for 1 h. Later the reactant was washed by using distilled water for 2–3 times, and the organic phase was dehydrated with anhydrous Na_2SO_4, and then purified by conducting column chromatography (dichloromethane: ethyl acetate: n-hexane = 1:0.5:5), and 367.3 mg red solids were obtained(yield 19.07%). ^1H NMR ($CDCl_3$, 600 MHz), δ(ppm): 1.46 (s, 6H), 2.56 (s, 6H), 6.02 (s, 2H), 7.33 (d, J = 6 Hz, 1H), 7.52 (d, J = 6.0 Hz, 1H), 8.10 (s, 1H), 10.70 (s, 1H); ^{13}C NMR (DMSO-d_6, 150 MHz), δ(ppm): 14.65, 15.10, 118.86, 121.21, 121.84, 125.02, 127.22, 131.56, 133.97, 137.25, 142.56, 155.33, 156.63;

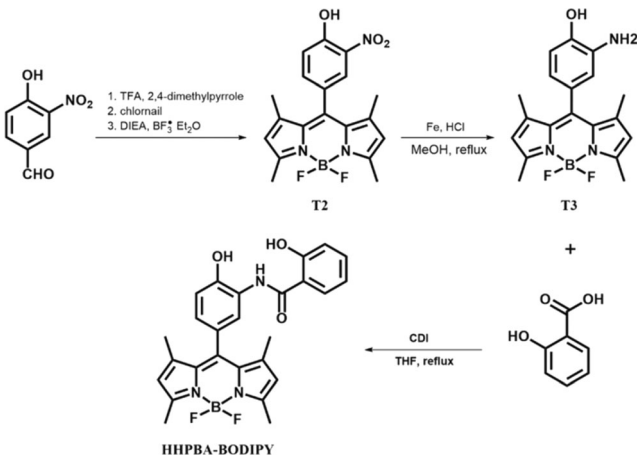

Scheme 1 Synthetic route of HHPBA-BODIPY

Synthesis of T3 T3 was synthesized basing on the method reported by Lu H. et.al. [36]. In 10 mL methanol a certain amount of compound T2 was dissolved, then 564.5 mg iron powder, 4 mL HCl solution (0.6 M) and 6 mL H_2O were added into the T2 solution and the resulting mixture was heated and mixed under reflux condition for 2 h. To monitor the process thin-layer chromatography(TLC) was applied. Later the product was cooled to room temperature naturally and centrifuged. After this, it was washed by using methanol several times until the supernatant was clear. Then, by using reduced pressure distillation the washing solution was removed, the products were separated through a silica gel column (dichloromethane: ethyl acetate: n-hexane = 1:1:5). The final product is 154.7 mg red solid with a yield of 77.8%. ^1H NMR (DMSO-d_6, 600 MHz) and δ(ppm): 1.51 (s, 6H), 2.41 (s, 6H), 4.74 (s, 2H), 6.12 (s, 2H), 6.28 (d, J = 6.0 Hz, 1H), 6.47 (s, 1H), 6.77 (d, J = 6 Hz, 1H), 9.43 (s, 1H); ^{13}C NMR (DMSO-d_6, 150 MHz), δ(ppm): 13.98, 14.14, 113.02, 114.76, 115.15, 120.87, 124.81, 131.08, 137.77, 142.77, 143.76, 144.59, 154.0.

Synthesis of HHPBA-BODIPY HHPBA-BODIPY was synthesized according to reported literature [37]. 81.1 mg carbonyl diimidazole was dissolved in 15 mL anhydrous tetrahydrofuran, then 69.1 mg salicylic acid was added. At room temperature the mixture reacted for 0.5 h under N_2 protection, then 195.3 mg compound T3 was added. After reacting at room temperature for 1 h, the mixture were heated under reflux condition, then the reaction continued around 24 h. To monitor the process TLC method was applied. When reaction finished, via rotary evaporation the solvent was removed, then the product was separated through a silica gel column (ethyl acetate: dichloromethane: petroleum ether = 1:1:5), and the component having a Rf of 0.13 was collected. Again to remove the solvent rotary evaporation was conducted and then the product was recrystallized (dichloromethane: n-hexane =

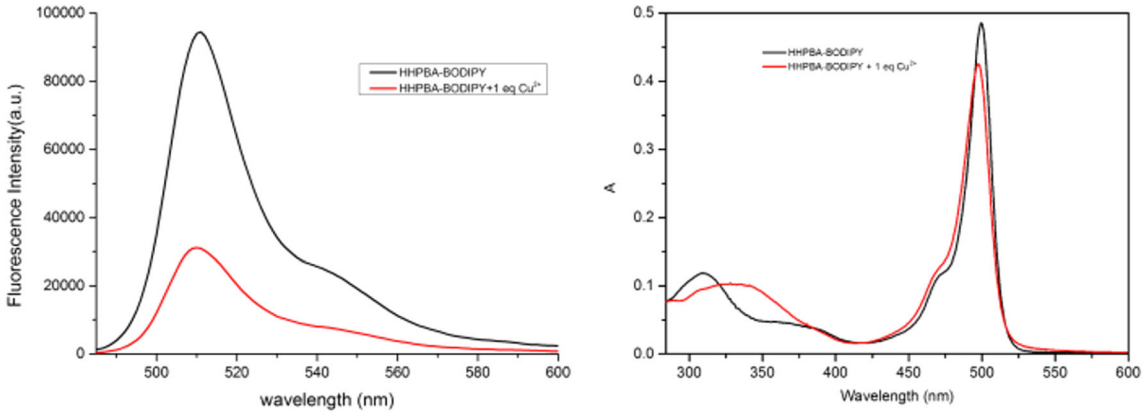

Fig. 1 The spectral changes of fluorescence emission spectra and UV-Vis absorption spectra after Cu^{2+} addition in HHPBA-BODIPY (5 μM) EtOH-HEPES solution(10 mM, 1/1, *v*/v, pH = 7.0, λex = 470 nm)

1:1) to afford compound HHPBA-BODIPY(75.5 mg with a yield of 35.16%). ^{1}H NMR (DMSO-d_6, 600 MHz), δ(ppm): 1.49 (s, 6H), 2.43 (s, 6H), 6.16 (s, 2H), 6.88 (d, J = 12 Hz, 2H), 6.95 (t, J = 6.0 Hz, 1H), 6.99 (d, J = 7 Hz, 1H), 7.06 (d, J = 6 Hz, 1H), 7.39 (t, J = 6 Hz, 1H), 7.96(d, J = 12 Hz, 1H), 8.28 (s, 1H), 10.56 (s, 1H), 10.91 (s, 1H), 11.71 (s, 1H); ^{13}C NMR (DMSO-d_6, 150 MHz), δ/ppm: 14.14, 14.17, 115.20, 116.80, 118.64, 119.57, 119.67, 121.13, 123.03, 124.31, 127.87, 130.67, 131.06, 133.33, 142.45, 142.69, 147.41, 154.47, 156.16, 163.48; HRMS (ESI), found:[M-H] + 474.1857, HHPBA-BODIPY requires [M-H] + 474.1801.

Results and Discussions

Synthesis

Based on the synthetic route showed in Scheme 1 HHPBA-BODIPY was synthesized and the product compound was characterized through HRMS, ^{1}H NMR and ^{13}C NMR (Fig. S1, S2, S3). These results attested that the amide, phenolic hydroxyl and carbonyl groups have been successfully attached to the BODIPY scaffold.

Spectroscopic Properties

The absorption and emission spectra of HHPBA-BODIPY are determined in EtOH solution, and its spectral shape is similar to that of most BODIPY fluorescent dyes. Normalized absorption and emission spectra of HHPBA-BODIPY are presented in Fig. S4. It has a strong absorption band at 499 nm (ε = 8.44×10^4 cm^{-1}•M^{-1}), and there is a weak absorption shoulder peak near 470 nm. The fluorescence emission spectrum showed a maximum intensity at 510 nm with a small Stokes shift of 11 nm, which corresponds to the S_1-S_0 transition of HHPBA-BODIPY. The quantum yield of the HHPBA-BODIPY fluorescent molecule, determined by using the integrating sphere measurement, was 0.06, and the fluorescence lifetime was 2.03 ns (45.46%), 0.4878 ns (54.54%).

Responses towards Cu^{2+}

When a certain amount of Cu^{2+} is added to the HHPBA-BODIPY solution, the spectral change is presented in Fig. 1, and the fluorescence emission at 510 nm is quenched. The absorption spectrum of HHPBA-BODIPY also changed after Cu^{2+} addition. The absorption peak at 499 nm was attenuated,

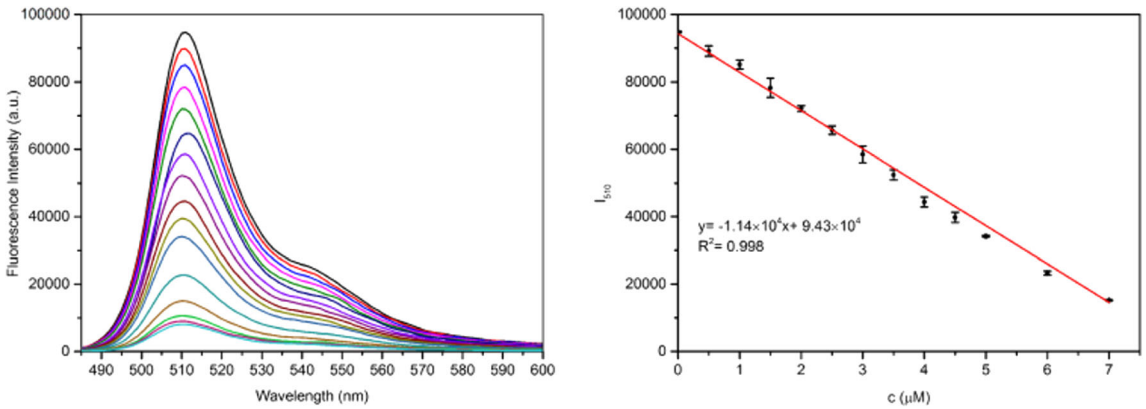

Fig. 2 The spectral changes of fluorescence emission spectra after the introduction of Cu^{2+} in HHPBA-BODIPY (5 μM) EtOH-HEPES solution (λex = 470 nm, pH = 7.0, 10 mM, 1/1, v/v) and the relationship between the Cu^{2+} content and the fluorescence intensity I_{510} at 510 nm

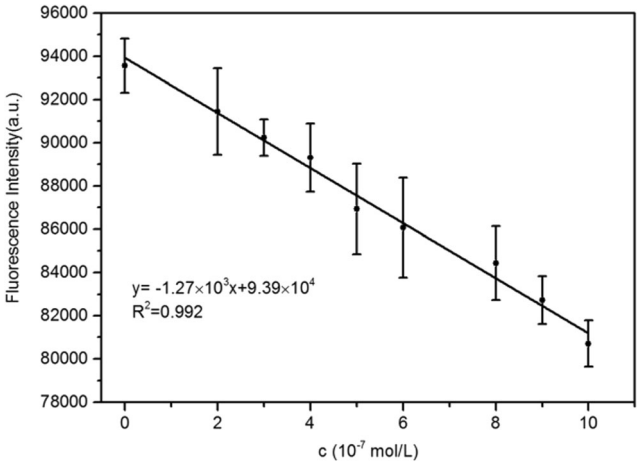

Fig. 3 The relationship betwee the Cu^{2+} concentration and the fluorescence intensity of HHPBA-BODIPY(5 μm) in EtOH-HEPES solution (10 mM, 1/1, v/v, λex = 47 0 nm, pH = 7.0) at low concentration

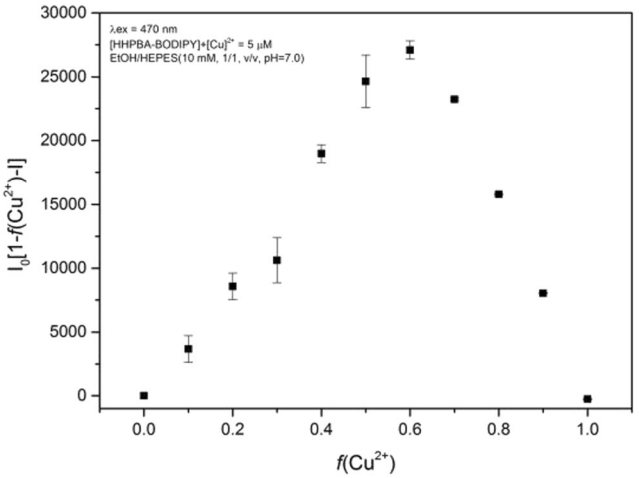

Fig. 5 Determine the coordinate number of HHPBA-BODIPY and Cu^{2+} by using the method of equivalent molarity ([HHPBA-BODIPY] + [Cu^{2+}] = 5 μM, λex = 470 nm)

and the maximum absorption wavelength blue-shifted to 497 nm. In ultraviolet region, the absorption band of HHPBA-BODIPY at 310 nm was attenuated, and the absorption peak at 330 nm is enhanced. These spectral changes indicate that the HHPBA-BODIPY probe molecule may coordinated with Cu^{2+}.

The fluorescence intensity at 510 nm shows a good linear relationship with the copper ion content (Fig.2). When the Cu^{2+} concentration is between 0 and 7.5 μM, the linear correlation coefficient $R^2 = 0.995$ ($n = 15$).

Detection Limit

Figure 3 shows the relationship between the copper ions concentration and the fluorescence intensity of HHPBA-BODIPY at low concentration. By measuring the standard deviation (Sb = 1450) of HHPBA-BODIPY without adding Cu^{2+}, the detection limit of HHPBA-BODIPY is 0.35 μM by using the equation [38](LOD = K × Sb/S), which indicates that HHPBA-BODIPY possesses good detection ability towards copper ions.

Reaction Mechanism

According to the variations of emission spectra and absorption spectra, the HHPBA-BODIPY coordination with Cu^{2+} may be the cause of the fluorescence quenching. Figure 4 exhibits that the probe molecule fluorescence intensity changes with Cu^{2+} equivalent added in HHPBA-BODIPY solution. When the Cu^{2+} concentration is greater than 1.5 times of the probe molecule concentration, with the copper ion addition, the probe molecule fluorescence intensity is essentially unchanged, and it can be inferred that the probe molecule is likely to be 1:1 coordinated with Cu^{2+}.

The method of equivalent molarity is often used to determine the coordination constant of a complex. For fluorescence

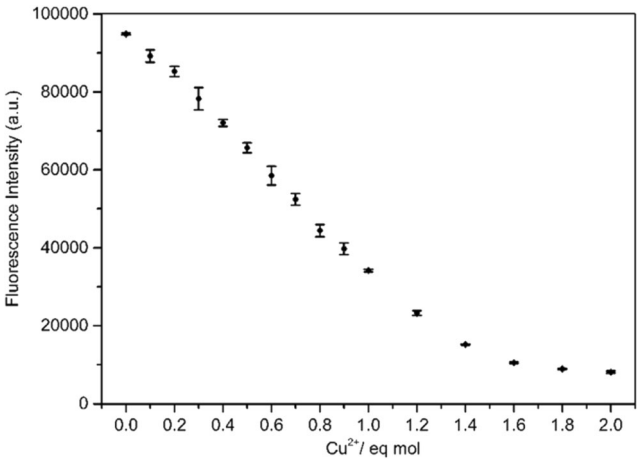

Fig. 4 The relationship between the intensity of HHPBA-BODIPY at 510 nm and the Cu^{2+} content in EtOH-HEPES solution (10 mM, 1/1, v/v, λex = 470 nm, pH = 7.0) with certain equivalent copper ions added

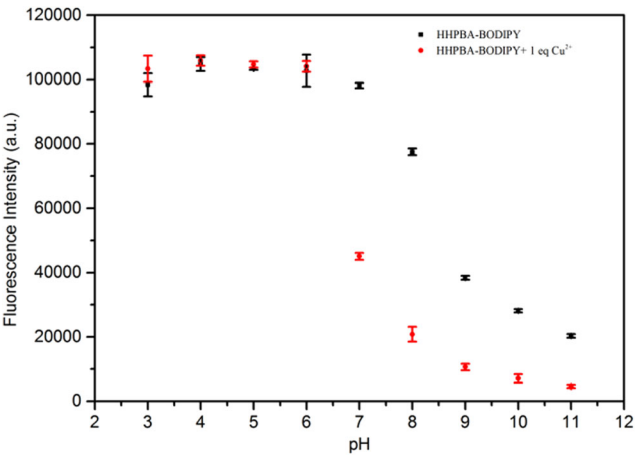

Fig. 6 The fluorescence emission intensity before and after adding 1 eq Cu^{2+} to HHPBA-BODIPY (5 μM) EtOH-HEPES solution (10 mM, λex = 470 nm, 1/1, v/v) under various pH conditions

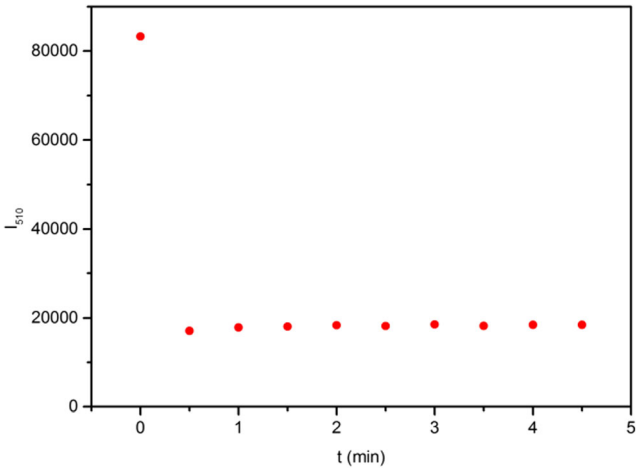

Fig. 7 The changes of fluorescence emission intensity with time after adding 1 eq Cu^{2+} to HHPBA-BODIPY (5 μM) EtOH-HEPES solution (10 mM, 1/1, v/v, λex = 470 nm, pH = 7.0)

quenching systems, the coordination number of the complex can also be determined using the deformation of the method of equivalent molarity [39]. Figure 5 shows the experimental results. It can be seen that the value of I_0[1-f(Cu^{2+})]-I is maximized when the relative content of Cu^{2+} is between 0.5 and 0.6, that is, the composition of the complex is ML or M_3L_2.The probe molecule HHPBA-BODIPY may form a 1:1 complex or a 2:3 complex during the identification of copper ions. ESI-MS analysis of the complex revealed a composition with a coordination ratio of 1:1 in the spectrum (Fig. S5) [Cu(HHPBA-BODIPY)] + (Cal:538.1175; Found: 538.1840), and the isotope analysis is also basically consistent with the calculated values.Therefore, HHPBA-BODIPY is most likely to coordinate with copper ions with a coordination ratio of 1:1 in the process of recognizing copper ions.

pH and Time Effect

pH value is an extremely important parameter for probe molecules. In this part the pH effect of HHPBA-BODIPY towards Cu^{2+} detection was explored. The results are presented in Fig. 6. The fluorescence intensity at 510 nm varies greatly with pH. Under acidic conditions, the probe molecule has a strong fluorescence emission, and the fluorescence intensity basically does not change with pH. When pH > 7, the fluorescence of the probe molecule gradually attenuates as the increase of solution alkalinity, and is finally almost completely quenched. After adding a certain amount of Cu^{2+}, the probe molecule has almost no response to Cu^{2+} when pH < 6, while the addition of Cu^{2+} can quench the fluorescence of HHPBA-BODIPY when pH > 6. The protonation of phenolic hydroxyl groups of HHPBA-BODIPY under acidic conditions may be related to this result. Under acidic conditions, the protonated phenolic hydroxyl group has weaker coordination ability and cannot chelate with Cu^{2+}, resulting in the consequence that the fluorescence of HHPBA-BODIPY molecules does not change with the addition of Cu^{2+}. As the alkalinity of the solution increases, phenolic hydroxyl groups begin to dissociate, and the ability of HHPBA-BODIPY to chelate with Cu^{2+} is enhanced, thereby quenching the fluorescence of HHPBA-BODIPY.

The response time is also an important indicator of the performance of the probe molecule. In general, it is desirable that the probe molecule respond as quickly as possible to the analyte. HHPBA-BODIPY responds very rapidly to Cu^{2+}, as shown in Fig. 7, after Cu^{2+} was added, the fluorescence of HHPBA-BODIPY is quickly quenched and remains stable during the measurement time. This characteristic of the probe can be used to real-time monitor the environmental samples.

Selectivity of HHPBA-BODIPY

Selectivity is another important performance indicator for fluorescent probe molecules. The selectivity of HHPBA-BODIPY probe towards Cu^{2+} was compared to other metal cations and was evaluated in this part. The results are shown in Fig. 8, that HHPBA-BODIPY showed no obvious response to cations including, Zn^{2+}, Mg^{2+}, Cd^{2+}, Al^{3+}, Pb^{2+}, Ni^{2+}, Hg^{2+},

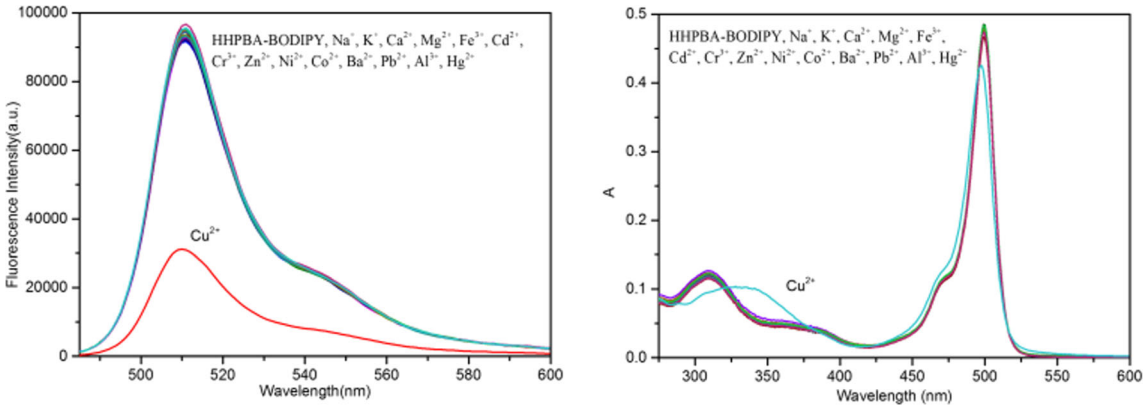

Fig. 8 Fluorescence and absorption spectra of HHPBA-BODIPY (5 μM) EtOH-HEPES solution (10 mM, 1/1, v/v, λex = 470 nm, pH = 7.0) after adding different metal cations

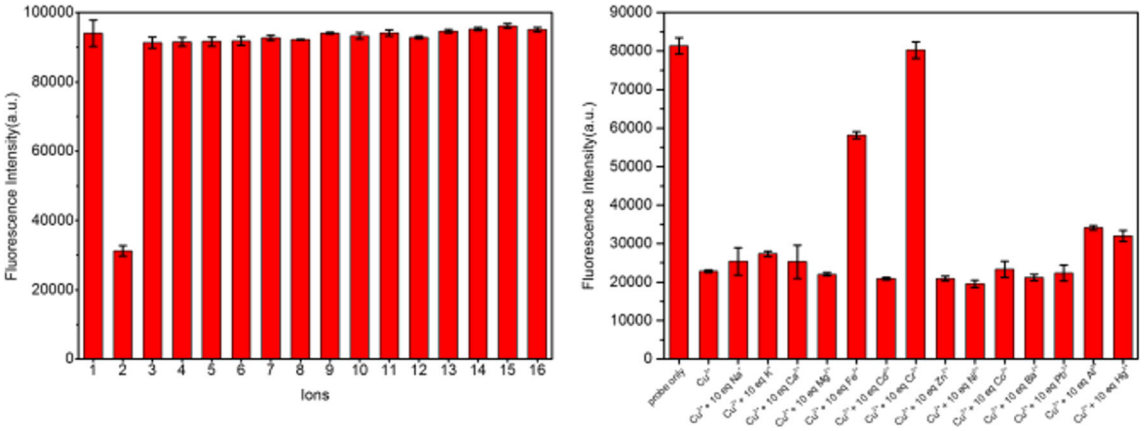

Fig. 9 (a) HHPBA-BODIPY Fluorescence intensity (5 μM) in EtOH-HEPES solution (10 mM, 1/1, v/v, λex = 470 nm, pH = 7.0) after adding 1 eq different metal cations 9(b) Fluorescence intensity of the probe molecule after adding of 1 eq Cu^{2+} in the presence of 10 eq of various cations. 1: HHPBA-BODIPY 2: Cu^{2+} 3: Na^{+} 4: K^{+}, 5: Ca^{2+} 6: Mg^{2+} 7: Fe^{3+} 8: Cd^{2+} 9: Cr^{3+} 10: Zn^{2+} 11: Ni^{2+} 12: Co^{2+} 13: Ba^{2+} 14: Pb^{2+} 15: Al^{3+} 16: Hg^{2+}

K^{+}. The introduction of these metal ions does not result significant changes to the fluorescence emission spectra and absorption spectra of HHPBA-BODIPY. The results of competitive experiments (Fig.9a and 9b) show that the presence of Zn^{2+}, Mg^{2+}, Cd^{2+}, Al^{3+}, Pb^{2+}, Ni^{2+}, Hg^{2+}, K^{+}, etc. exhibited no interference, except Fe^{3+} and Cr^{3+}.

After adding Cu^{2+} in the presence of Fe^{3+}, the fluorescence intensity of HHPBA-BODIPY was weakened, but the degree of attenuation is significantly lower than that without iron ions. The appearance of Cr^{3+} also showed a significant impact. In the presence of 10 times of Cr^{3+} ions, HHPBA-BODIPY has little response to Cu^{2+}.

Cu^{2+} Detection in Water Samples

To investigate whether HHPBA-BODIPY can be used for real-time analysis of environmental samples, tap water and yellow river water were selected in this section. By adding a certain concentration of Cu^{2+} solution, the detection ability of HHPBA-BODIPY fluorescent molecular probe was measured.The results are shown in Table 1. Obviously that the probe molecule exhibits a good yield of copper ions added to tap water sample between 4 and 12 μM. Though the detection sensitivity towards Cu^{2+} in the Yellow River water is not as good as that in tap water, the probe still showed good yields in the low concentration range. According to the experimental results, HHPBA-BODIPY probe possesses the potential for environmental sample analysis and monitoring.

Conclusion

In this work, the fluorescent molecular probe HHPBA-BODIPY possessing phenolic hydroxyl group and amide group was synthesized by using fluoroboron pyrrole fluorophore as skeleton and 2-hydroxy-N-(2-hydroxyphenyl)benzamide as the recognition unit.Then, the photophysical properties of the HHPBA-BODIPY fluorescent probe molecule were determined. The experimental results of Cu^{2+} recognition showed that the HHPBA-BODIPY probe resulted in fluorescence quenching by coordination with Cu^{2+}. Thereby the Cu^{2+} concentration can be determined through measuring the fluorescence emission intensity of HHPBA-BODIPY, which showed a good linear relationship.

Table 1 Cu^{2+} detection results of HHPBA-BODIPY in tap water and Yellow River water samples

Sample	Cu^{2+} added / μM	Results* / μM	Recovery rate (%)
Tap water 1	0.00	0.92 ± 0.10	/
Tap water 2	4.00	3.73 ± 0.06	93.3
Tap water 3	8.00	7.43 ± 0.10	92.8
Tap water 4	12.00	10.8 ± 0.19	89.6
Yellow River water 1	0.00	0.30 ± 0.46	/
Yellow River water 2	4.00	3.72 ± 0.22	93.1
Yellow River water 3	8.00	6.75 ± 0.24	84.4
Yellow River water 4	12.00	9.72 ± 0.09	81.0

*Average results of three measurements ± Standard deviation

The HHPBA-BODIPY probe can respond to Cu^{2+} rapidly under near-neutral conditions, and showed good detection ability towards Cu^{2+} in the concentration range of 0.35-7 μM. Furthermore, the presence of most metal cations does not influence Cu^{2+} recognition, except Fe^{3+} and Cr^{3+}. The analysis results of water samples also showed that HHPBA-BODIPY possesses the potentiality in real sample determination.

Acknowledgements This work was supported by National Natural Science Foundation of China (21876073).

References

1. Kim B-E, Nevitt T, Thiele DJ (2008) Mechanisms for copper acquisition, distribution and regulation. Nat Chem Biol 4(3):176–185
2. Pena MM, Lee J, Thiele DJ (1999) A delicate balance: homeostatic control of copper uptake and distribution. J Nutr 129(7):1251–1260
3. Jomova K, Valko M (2011) Advances in metal-induced oxidative stress and human disease. Tosicology. 283(2):65–87
4. Svetlana L, Barnes NL, Bartee MY, Dmitriev OY (2007) Function and regulation of human copper-transporting ATPases. Physiol Rev 87(3):1011–1046
5. Elena G, Henryk K, Daniela V, Gianni V (2010) Copper homeostasis and neurodegenerative disorders (Alzheimer's, prion, and Parkinson's diseases and amyotrophic lateral sclerosis). Chemical Reviews; 37(37):no-no.
6. Rossi L, Arciello M, Capo C, Rotilio G (2006) Copper imbalance and oxidative stress in neurodegeneration. Ital J Biochem 55(3–4): 212
7. Sharma AK, Pavlova ST, Kim J, Kim J, Mirica LM (2013) The effect of Cu^{2+} and Zn^{2+} on the Aβ42 peptide aggregation and cellular toxicity. Metallomics Integrated Biometal Science 5(11): 1529–1536
8. Zhang Z, Liu Y, Wang E (2019) A highly selective "turn-on" fluorescent probe for detecting Cu^{2+} in two different sensing mechanisms. Dyes Pigments 163:533–537
9. Lushchak VI (2011) Environmentally induced oxidative stress in aquatic animals. Aquat Toxicol 101(1):13–30
10. Schamphelaere KAC (2002) De, Janssen CR. A biotic ligand model predicting acute copper toxicity for Daphnia magna: the effects of calcium, magnesium, sodium, potassium, and pH. Environmental Science & Technology 36(1):48–54
11. Xiaowei C, Weiying L, Kaibo Z, Longwei H (2012) A near-infrared fluorescent turn-on probe for fluorescence imaging of hydrogen sulfide in living cells based on thiolysis of dinitrophenyl ether. Chem Commun 48(85):10529–10531
12. Liu J, Yue Y, Wang J, Yan X, Liu R, Sun Y, Li X (2015) Study of interaction between human serum albumin and three phenanthridine derivatives: Fluorescencespectroscopy and computational approach. Spectrochim Acta A Mol Biomol Spectrosc 145: 473–481
13. Domaille DW, Que EL Chang CJ. Synthetic fluorescent sensors for studying the cell biology of metals
14. Chen H, Sun T, Qiao XG, Tang QO, Zhao SC, Zhou Z (2018) Red-emitting fluorescent probe for detecting hypochlorite acid in vitro and in vivo. Spectrochimica Acta Part A Molecular & Biomolecular Spectroscopy. 204:196–202
15. Young-Keun Y, Keun-Jeong Y, Jinsung T (2005) A rhodamine-based fluorescent and colorimetric chemodosimeter for the rapid detection of Hg^{2+} ions in aqueous media. J Am Chem Soc 127(48):16760–16761
16. Zhaochao X, Juyoung Y, Spring DR (2010) Fluorescent chemosensors for Zn^{2+}. Chem Soc Rev 39(6):1996–2006
17. Weissleder R, Tung CH, Mahmood U, Bogdanov A (1999) In vivo imaging of tumors with protease-activated near-infrared fluorescent probes. Nat Biotechnol 17(4):375–378
18. Hisataka K, Mikako O, Raphael A, Choyke PL, Yasuteru U (2010) New strategies for fluorescent probe design in medical diagnostic imaging. Chem Rev 110(5):2620–2640
19. Yue Y, Yin C, Huo F, Chao J, Zhang Y (2016) Thiol-chromene click chemistry: a turn-on fluorescent probe for specific detection of cysteine and its application in bioimaging. Sensors & Actuators B Chemical. 223(2):496–500
20. Vernekar SKV, Hallaq HY, Guy C, Thompson AJ, Linda S, Lummis SCR et al (2010) Toward biophysical probes for the 5-HT3 receptor: structure-activity relationship study of granisetron derivatives. J Med Chem 53(5):2324–2328
21. Belousov V, Fradkov A, Lukyanov K, Staroverov D, Shakhbazov K (2006) Av, Lukyanov S. genetically encoded fluorescent indicator for intracellular hydrogen peroxide. Nat Methods 3(4):281–286
22. Liu J, Liu C, He W (2013) Fluorophores and their applications as molecular probes in living cells. Curr Org Chem 17(6):564–579
23. Dujols V, Czarnik AW (1997) A Long-wavelength fluorescent Chemodosimeter selective for cu(II) ion in water. J Am Chem Soc 119(31):7386–7387
24. Yu X, Zifan L, Xiaotong C, Aijun T (2008) Highly sensitive and selective optical chemosensor for determination of Cu^{2+} in aqueous solution. Talanta. 74(5):1148–1153
25. Liang H, Xiao W, Guoqiang X, Pinxian X, Zhengpeng L, Min X et al (2010) A new rhodamine-based chemosensor for Cu^{2+} and the study of its behaviour in living cells. Dalton Trans 39(34):7894–7896
26. Ying Z, Fang W, Youngmee K, Sung-Jin K, Juyoung Y (2009) Cu^{2+}-selective ratiometric and "off-on" sensor based on the rhodamine derivative bearing pyrene group. Org Lett 11(19):4442–4445
27. Wang Y, Chang HQ, Wu WN, Peng WB, Yan YF, He CM, Chen TT, Zhao XL, Xu ZQ (2016) Rhodamine 6G hydrazone bearing pyrrole unit: Ratiometric and selective fluorescent sensor for Cu^{2+} based on two different approaches. Sensors & Actuators B Chemical 228:395–400
28. Chen Z (2013) Wang, Limin, Zou, gang, et al. highly selective fluorescence turn-on chemosensor based on naphthalimide derivatives for detection of copper(II) ions. Spectrochimica Acta Part A Molecular & Biomolecular Spectroscopy 105(105C):57–61
29. Cristina S, Giuseppe Trusso S, Maria Emanuela A, Ballistreri FP, Agata C, Maria Laura G et al (2013) A ratiometric naphthalimide sensor for live cell imaging of copper(I). Chem Commun 49(49): 5565–5567
30. Zhang S, Yu T, Sun M, Yu H, Zhang Z, Wang S, Jiang H (2014) Highly sensitive and selective fluorescence detection of copper (II) ion based on multi-ligand metal chelation. Talanta. 126(126):185–190
31. Hee LM, Hyun Jung K, Sangwoon Y, Noejung P, Jong SK (2008) Metal ion induced FRET OFF-ON in tren/dansyl-appended rhodamine. Org Lett 10(2):213–216
32. Noel B, Volker L, Wim D (2012) Fluorescent indicators based on BODIPY. Chem Soc Rev 41(3):1130–1172
33. Kowada T, Maeda H, Kikuchi K (2015) BODIPY-based probes for the fluorescence imaging of biomolecules in living cells. Chem Soc Rev 44(14):4953–4972
34. Yu G, Tasuku U, Yasuteru U, Hirotatsu K, Tetsuo N (2006) Tunable design strategy for fluorescence probes based on 4-substituted BODIPY chromophore: improvement of highly

sensitive fluorescence probe for nitric oxide. Analytical & Bioanalytical Chemistry 386(3):621–626
35. Wakamiya A, Murakami T, Yamaguchi S (2013) Benzene-fused BODIPY and fully-fused BODIPY dimer: impacts of the ring-fusing at the b bond in the BODIPY skeleton. Chem Sci 4(3): 1002–1007
36. Hua L, Zhaoli X, John M, Zhen S, Xiaozeng Y, Nagao K (2010) Specific Cu^{2+}-induced J-aggregation and Hg^{2+}-induced fluorescence enhancement based on BODIPY. Chem Commun 46(20): 3565–3567
37. Kumar A, Narasimhan B, Kumar D (2007) Synthesis, antimicrobial, and QSAR studies of substituted benzamides. Bioorg Med Chem 15(12):4113–4124
38. Long GL, Winefordner JD (1983) Limit of detection. A closer look at the IUPAC definition. Anal Chem 55(7):712–724
39. Chen F, Hou F, Huang L, Cheng J, Liu H, Xi P, Bai D, Zeng Z (2013) Development of a novel fluorescent probe for copper ion in near aqueous media. Dyes Pigments 98(1):146–152